Diurnal and Seasonal Variation of Clear-Sky Land Surface Temperature of Several Representative Land Surface Types in China Retrieved by GMS-5*

WANG Minyan[1,2] (王旻燕) and Lu Daren[2] (吕达仁)

1 *National Meteorological Information Center, China Meteorological Administration, Beijing* 100081

2 *LAGEO, Institute of Atmospheric Physics, Chinese Academy of Sciences, Beijing* 100029

(Received October 30, 2006)

ABSTRACT

The retrieved results in this paper by GMS-5/VISSR thermal infrared data with single time/dual channel Split-Window Algorithm reveal the characteristics of diurnal and seasonal variation of clear-sky land surface temperature (LST) of several representative land surface types in China, including Tarim Basin, Qinghai-Tibetan Plateau, Hunshandake Sands, North China Plain, and South China. The seasonal variation of clear-sky LST in above areas varies distinctly for the different surface albedo, soil water content, and the extent of influence by solar radiation. The monthly average diurnal ranges of LST have two peaks and two valleys in one year. The characteristics of LST in most land of East Asia and that of sea surface temperature (SST) in the south of Taiwan Strait and the Yellow Sea are also analyzed as comparison. Tarim Basin and Hunshandake Sands have not only considerable LST diurnal cycle but also remarkable seasonal variation. In 2000, the maximum monthly average diurnal ranges of LST in both areas are over 30 K, and the annual range in Hunshadake Sands reaches 58.50 K. Seasonal variation of LST in the Qinghai-Tibetan Plateau is less than those in East Asia, Tarim Basin, and Hunshandake Sands. However, the maximum diurnal range exists in this area. The yearly average diurnal range is 28.05 K in the Qinghai-Tibetan Plateau in 2000. The characteristics of diurnal, seasonal, and annual variation from 1998 to 2000 are also shown in this research. All the results will be valuable to the research of climate change, radiation balance, and estimation for the change of land surface types.

Key words: GMS-5, land surface temperature (LST), diurnal and seasonal variation

1. Introduction

Regional LST (land surface temperature) is an important climate factor. LST not only indicates the influence of solar radiation and the atmosphere on land surface but also represent the heat properties of land surface, relating to the land surface type, moisture, and hydrologic-thermal equilibrium. The characteristics of regional LST and its diurnal variation through remote sensing are crucial for climate simulation and validation.

The development of land surface model requires a higher temporal-spatial resolution and accuracy of LST. LST as well as the difference between LST and the surface air temperature has great impact on the exchange of energy flux, water vapor flux on the land-atmosphere interface. Coupled land-atmosphere climate model (SVAT: soil/vegetable/atmosphere transfer) usually takes the surface air temperature as the temperature of the land surface, which has a big limitation in the field. However, to retrieve LST by split-window algorithm with a high feasibility of RMSE (Root Mean Square Error) of 2-4 K (Price, 1984; Becker and Li, 1990, 1995; Prata and Platt, 1991; Ulivieri and Castromuovo, 1994; Prata and Cechet, 1999) can improve it. Round-the-clock LST dataset is necessary for model evaluation. Furthermore, it can be used to study the energy equilibrium of the land-atmosphere system by considering the relationship between LST and the sensible/latent heat flux.

In the work of Jin (1997), the global LST during 1981-1998 is retrieved with NOAA/AVHRR data, and night LST is computed by the coupled model of NCAR CCM3 (Climate Community Model) & BATS (Biosphere Atmosphere Transfer Scheme), with consideration of the air temperature variation at night as

*Supported jointly by the National Facilities and Information Infrastructure for Science and Technology Project (2005DKA31700) and the National Nature Science Foundation of China (Nos. 40333034 and 49790020).

reference. The advantage of geostationary meteorological satellite is to monitor real-time and continuous variation of the earth-atmosphere system in the same large area, which offsets the disadvantage of polar satellites in the aspects of remote sensing on diurnal variation of parameters in the earth-atmosphere system. The rules of diurnal, seasonal, and annual variation of regional LST reflect different extent of influences on various land surface types by solar radiation, land surface albedo, soil thermal inertia, heat exchange with air, and other integrated factors. The characteristics of spatial distribution, diurnal range, and long-term variation of LST in a large area play a significant role in land monitoring, as well as climate and environment analysis.

For a long period, the regional GIS (Geographic Information System) database usually comprises atmospheric temperature data information, such as yearly and monthly average air temperature, annual and diurnal range of air temperature with high accuracy, which is easier to measure and is influenced less by other factors during the measurement. An algorithm with adequate accuracy and longer time series to acquire LST can complement the GIS database with the 10-day, monthly, yearly average LST values and their variations. There are few studies now on the LST retrieval in China, except Yan et al. (2001), Oku and Ishikawa (2004), and so on, especially the application of LST. More efforts are in demand in this field.

By a single time/dual channel split-window algorithm which is validated to retrieve LST, the characteristics of diurnal, seasonal, and annual variations of LST of several representative land surface types in East Asia during 1998-2000 (mainly in 2000), the relationship between them and the key influential factors are studied in this paper. The difference of LST between Hunshandake Sands and Xilinguole typical grassland is also analyzed.

2. Theory and method

2.1 *Radiative transfer equation*

On the condition of local thermodynamic equilibrium in clear sky, assuming that the earth's surface is a Lambertian emitter and that the atmosphere is non-scattering, then radiation measured by a thermal infrared sensor (10-14 μm) aboard satellite in channel i is:

$$\begin{aligned} L_i(T_{\mathrm{b}i},\theta) &= \varepsilon_i\tau_i(\theta)B_i(T_{\mathrm{s}}) + L_i(\theta)\uparrow \\ &\quad +(1-\varepsilon_i)\tau_i(\theta)L_i(\theta)\downarrow \qquad i=1,2, \end{aligned} \tag{1}$$

where $T_{\mathrm{b}i}$ is brightness temperature measured in channel i, ε_i is surface emissivity in this channel, $\tau_i(\theta)$ is atmospheric transmittance at zenith angle θ from the ground to the top of the atmosphere, $B_i(T_{\mathrm{s}})$ is blackbody spectral radiance of the ground in channel i with land surface temperature T_{s}, and $L_i(\theta)\uparrow$ is upward radiation emitted by the atmosphere. The third term on the right of Eq.(1) represents that the downward radiation $L_i(\theta)\downarrow$ emitted by the atmosphere is reflected by the ground $(1-\varepsilon_i)$ toward satellite with attenuation of the atmosphere.

If surface emissivity is known in clear sky, $L_i(\theta)\uparrow$, $L_i(\theta)\downarrow$, and $\tau_i(\theta)$ can be computed by atmospheric RTE (Radiative Transfer Equation) with real-time sounding profile, after the spectral response correction, the final solution can be derived. Single time/dual channels split-window algorithm makes use of the infrared information of the adjacent atmospheric window channels. In order to get the reasonable solutions of Eq.(1) in both 10.5-11.5 μm and 11.5-12.5 μm of GMS-5/VISSR (Visible and Infrared Spin Scan Radiometer), a cost function J is necessary, as shown in Eq.(2), e_1 and e_2 are the difference between the left and right terms of Eq.(1) when i=1, 2, respectively. Iteration begins from the initial guess of brightness temperature in channel 10.5-11.5 μm, till it reaches the least cost function J. Normalization uses the average upward radiance of the atmosphere in two channels. Through numerical computation and comparative analysis, it shows that $J \leqslant 0.025$ is the best convergence criterion with most reasonable of the coefficients' matrix of known parameters to get the unique solution.

$$J = \frac{\sqrt{e_1^2+e_2^2}}{(L_1(T_{\mathrm{b}1},\theta)+L_2(T_{\mathrm{b}2},\theta))/2}. \tag{2}$$

2.2 *Solution of the RTE*

In cloudy FOV (Field of View), satellite sensor measures radiation emitted by clouds. But in clear sky, the measured brightness temperature is from the radiation emitted by the ground. Therefore, cloud detection must be done before LST retrieval. Brightness temperatures of cloud and land surface vary differently. Temporal/spatial variation of cloud is higher than that of land surface. Considering of this, the identification of clear sky pixel is the first step to retrieve LST. In this research, spatial-temporal threshold criterion (Mao et al., 1999) is used for clear sky detection.

To derive the surface emissivity ε with NOAA/AVHRR derived NDVI data with daily 8-km resolution, an "NDVI-ε" method used by Sobrino and Raissouni (2000) to analyze the relationship between the surface emissivity and NDVI is employed to define surface emissivity in this research. On the basis of MVC (maximum value composite), maximum NDVI of each pixel per 10 days is taken to eliminate the influences from cloud, atmosphere, and measuring angle. This method resolves a problem of missing data for no satellite measuring over some area in some days.

Within the GMS-5 satellite FOV (7°-66°N, 50°-180°E), observations were made twice per day at 00:00 and 12:00 GMT in the onshore sounding stations. GMS-5 geostationary satellite data have a spatial resolution of 12 km and a temporal resolution of 1 h. The parameters such as atmospheric transmittance, upward/downward radiation of the atmosphere in the RTE are computed from MODTRAN3.5 (Moderate Resolution and Radiative Transfer Model). When visibility data are available in some stations, the default visibility is replaced by the real-time one.

Generally, when the precipitable water in the atmosphere is less than 2.5 g cm^{-2} and the average atmospheric temperature is lower than 290 K, better LST retrieval results can be derived (Faysash and Smith, 1999). Therefore, it is defined to retrieve LST in this research: (1) clear sky, (2) the precipitable water in the atmosphere is less than 4.0 g cm^{-2} (derived from sounding profiles), and (3) relative humidity on the ground is less than 90%. Otherwise, it is not easy to get suitable solutions of RTE, or the value of atmospheric correction is unreasonably high than usual.

3. Validation

Satellite retrieved LST is composed of the average radiant brightness temperatures in satellite FOV of each pixel. One way to validate the retrieved LST is to compare the retrieval result with the observed temperature measured on the ground, such as observed 0-cm temperature on the ground or contact temperature transducer (CTT). The other way is to compare with the results from instruments in some field experiments (usually observing with radiative instruments during enhanced observation period), e.g., pyrgeometer, IR thermometer, etc. The latter, observation from some radiative instruments is hard to acquire. Thus observed 0-cm temperature on the ground at some meteorological stations are used for validation in this paper. Terra/MODIS LST product are also used for comparison as an indirect validation.

3.1 *Comparison with observed 0-cm temperature on the ground at Station No.* 54511

Result of comparison the retrieved LST with observed 0-cm temperature on the ground at Station No. 54511 (Beijing) with 151 samples in 2000 shows that the average error is 0.36 K, absolute error is 2.37 K, RMS (root mean square) error/bias (standard deviation) is 2.95 ±1.86 K, and the correlation coefficient reaches 0.947. The comparative analysis of the algorithm in this research with some improved split-window algorithms (Price, 1984; Becker and Li, 1990, 1995; Prata and Platt, 1991; Ulivieri et al., 1994; Prata and Cechet, 1999) shows that physical method in this research is better than others (Wang and Lu, 2005b).

3.2 *Comparison with observed* 0*-cm temperature on the ground at* 43 *national reference climatological stations in China*

The comparison with observed 0-cm temperature on the ground at 43 national reference climatological stations in China in 2000 includes 4720 samples in 2000. It shows that the average error is 0.18 K, absolute error is 3.50 K, and RMSE/bias is

4.31±4.30 K. Table 1 presents the time distribution of the errors between retrieved LST and observation, sample amount in each month, monthly average errors, and monthly absolute errors included. In the summer, samples are fewer with higher error. There are 32 stations (74.4% of total 43 stations) of which yearly average errors are within 2 K and maximum error of 3.49 K, 35 stations (81.4% of total 43 stations) of which yearly absolute error are within 4 K and maximum absolute error of 5.38 K. Absolute error in southwestern China is smaller, which may be related with the limitation of the atmospheric precipitable water less than 4 g cm^{-2}.

Table 1. Monthly average LST error (K) comparing retrieved results with observation in 43 stations in 2000

Month	1	2	3	4	5	6	7	8	9	10	11	12
Sample	795	692	597	360	199	104	56	62	168	285	571	831
$\overline{\varepsilon}$	0.48	-0.1	-1.1	-1.5	-0.9	-0.7	-3.8	-2.8	-0.5	0.38	1.66	1.69
$\lvert\overline{\varepsilon}\rvert$	2.83	3.26	3.87	4.33	5.24	5.57	6.07	4.74	4.36	3.31	3.11	2.95

3.3 *Comparison with MODIS LST products*

Terra/LST product with a temporal resolution of 5 min and spatial resolution of 1 km is from MODIS (MODerate resolution Imaging Spectrometer) day/night LST algorithm. LST products during the passing period of the polar satellite Terra (12:20-13:25 GMT) are compared with retrieved results at 12:00 with the algorithm in this paper. The samples exist only in the three provinces onshore northeast of China, Korea and Japan. From February to December in 2000, 129 pairs of LST results are available (pixels for comparison are within 15 km, excluding the samples with GMS-5/VISSR IR channel raw brightness temperature higher than MOD11_L2 V004 LST product in that retrieval value would be higher than the raw brightness temperature). Figure 1 shows that these two match perfectly, the correlation reaches 0.9811, and average absolute error is 2.84 K. Single time/dual channel split-window algorithm can meet the demands to study the characteristics of LST at a certain hour or medium/long term, LST variation, the interaction with other factors as well.

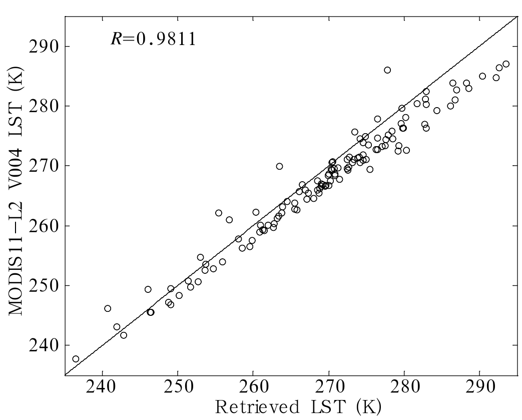

Fig.1. LST error (unit: K) scatter diagram comparing retrieval results with MOD11_L2 products in 2000 (unit: K).

4. Characteristics of LST variation

The diurnal variation of LST is a result of a diurnal variation of heating from solar radiation on the earth-atmosphere system as well as the physical properties of the land surface itself. The variation of LST is closely related to the short-wave reflectivity, long-wave emissivity, thermal inertia of the soil-vegetation system and heat exchange on the interface between the earth and the atmosphere, and greatly influenced by land surface type, soil moisture, and wind field.

4.1 *Selection of land surface types*

Several representative land surface types are analyzed in this paper to show the characteristics of diurnal variation of LST in China (Fig.2), i.e., the Tarim Basin (37.5°-40°N, 77°-85°E), the Qinghai-Tibetan Plateau (30.3°-36°N, 80°-95°E), the Hunshandake Sands (42.1°-43.5°N, 113°-116.31°E) and North China Plain (35°-40°N, 115°-122.5°E), South China (24°-25.45°N, 113.8°-115.6°E), part of land in East Asia (20.3°-54.2°N, 75.5°-130.3°E) excluding the sea. The SST in the south of Taiwan Strait (20.12°-21.56°N, 118.42°-120.3°E) and Yellow Sea (32°-34.2°N, 121.58°-126°E) are compared as well.

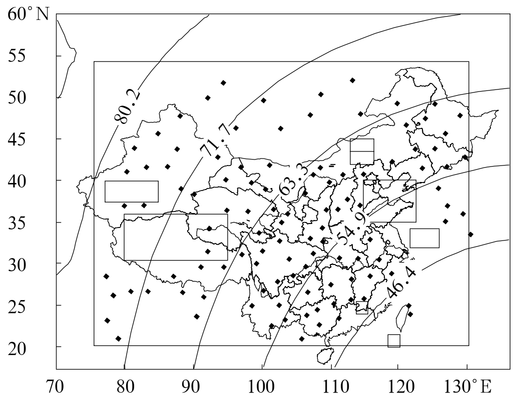

Fig.2. Distribution of focused representative surface types (sea excluded) and 143 sounding stations in East Asia. The contour lines are satellite zenith angle of GMS-5.

Southern Jiangxi Province and northern Guangdong Province with flat altitude of 250-500 m are selected from South China.

Yellow Sea area is adjacent to the coast. The sea in the south of Taiwan Strait is some distance away from the land. SST is calculated with reference to McClain method (McClain et al., 1985), and the brightness temperature of the corresponding channels is replaced by those of two GMS-5/VISSR IR channels. Equation (3) is used for the sea in the south of Taiwan Strait at 6:00-18:00 BT (Beijing Time) in daytime and Yellow Sea at 5:00-17:00 BT, from January to April and November to December. Equation (4) is used at night. In other months, add and subtract one hour to calculate LST in daytime.

$$T_{\rm SST} = 1.035T_{10.8} + 3.046(T_{10.8} - T_{11.9}) - 10.78(\text{day}), \quad (3)$$

$$T_{\rm SST} = 1.076T_{10.8} + 3.168(T_{10.8} - T_{11.9}) - 23.08(\text{night}). \quad (4)$$

4.2 *Diurnal and seasonal variations of LST in several representative land surface types in "pure" clear days in* 2000

In the study of diurnal and seasonal variation of LST, in order to avoid the uncertainty of cloud-radiation forcing in the earth-atmosphere system, only "pure" clear pixels are effective, which are determined as clear by using temporal-spatial criterion in all 24 h a day. Only these pixels have not been covered by cloud, thus they are useful to study the influence only by the factors like solar radiation, surface albedo, soil thermal inertia, and heat exchange.

Raw brightness temperature in 24 h is derived from average brightness temperature in clear regions, added by average atmospheric temperature correction (the difference between retrieved LST in the sounding stations and raw brightness temperature) in 00:00 and 12:00 GMT, then the temperature correction in other 22 h except 00 and 12 are derived by interpolation of the atmospheric temperature correction. It is well known that lower clouds reflect the solar short-wave radiation upward to decrease the radiation reaching ground, while higher clouds reflect the surface long-wave radiation downward to increase the radiation reaching the ground. Therefore, selection of "pure" clear pixels makes the study of diurnal cycle of LST out of interference of complicated cloud feedbacks.

Figure 3a shows the diurnal cycle of yearly average LST (24 h) in most land in East Asia in 2000. The LST variation gradient in daytime is larger than at night due to the impact of solar radiation (vertical distance between two circles in Fig.3a). The temperature increases sharply at 00:00 GMT (hereinafter) and reaches the peak at 05:00 when the temperature variation gradient is not large. Afterward, the temperature declines rapidly. The decline scale of LST after 12:00 becomes less, and the LST variation gradient is slight during the night and reaches a minimum in 21:00. Figure 3b describes the diurnal variations of LST in different months. The middle line refers to monthly average LST, which clearly reflects the characteristic of seasonal variation of LST in the land of East Asia at middle latitudes: warm in summer while cold in winter.

Figure 4 shows the diurnal and seasonal variation of monthly average LST/SST in the Tarim Basin, Qinghai-Tibetan Plateau, Hunshandake Sands, North China Plain, South China, most land in East Asia, sea in the south of Taiwan Strait, and Yellow Sea in 2000. The amplitude of each curve reveals the degree of the diurnal variation of LST/SST in the month. Twelve curves show the seasonal variation, of which the

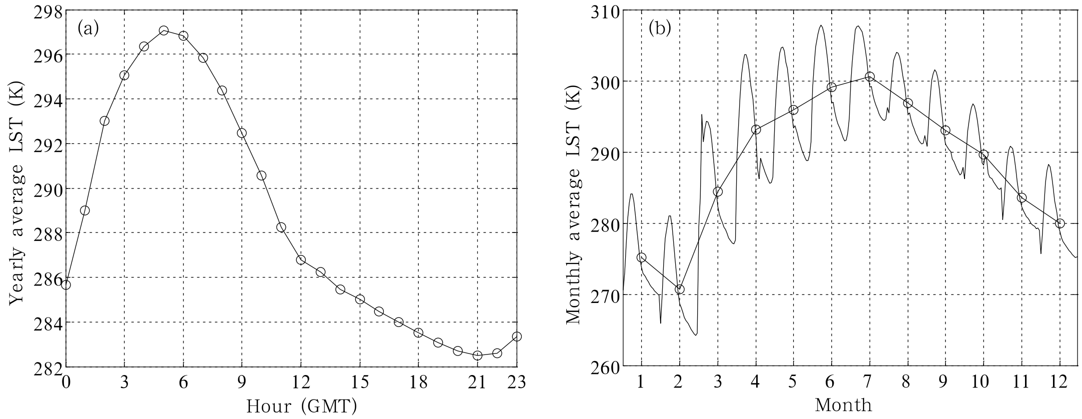

Fig.3. Diurnal cycle of yearly average LST (a) and seasonal variation of monthly average LST (b) diurnal cycle (K) in "pure" clear days in part of East Asia in 2000.

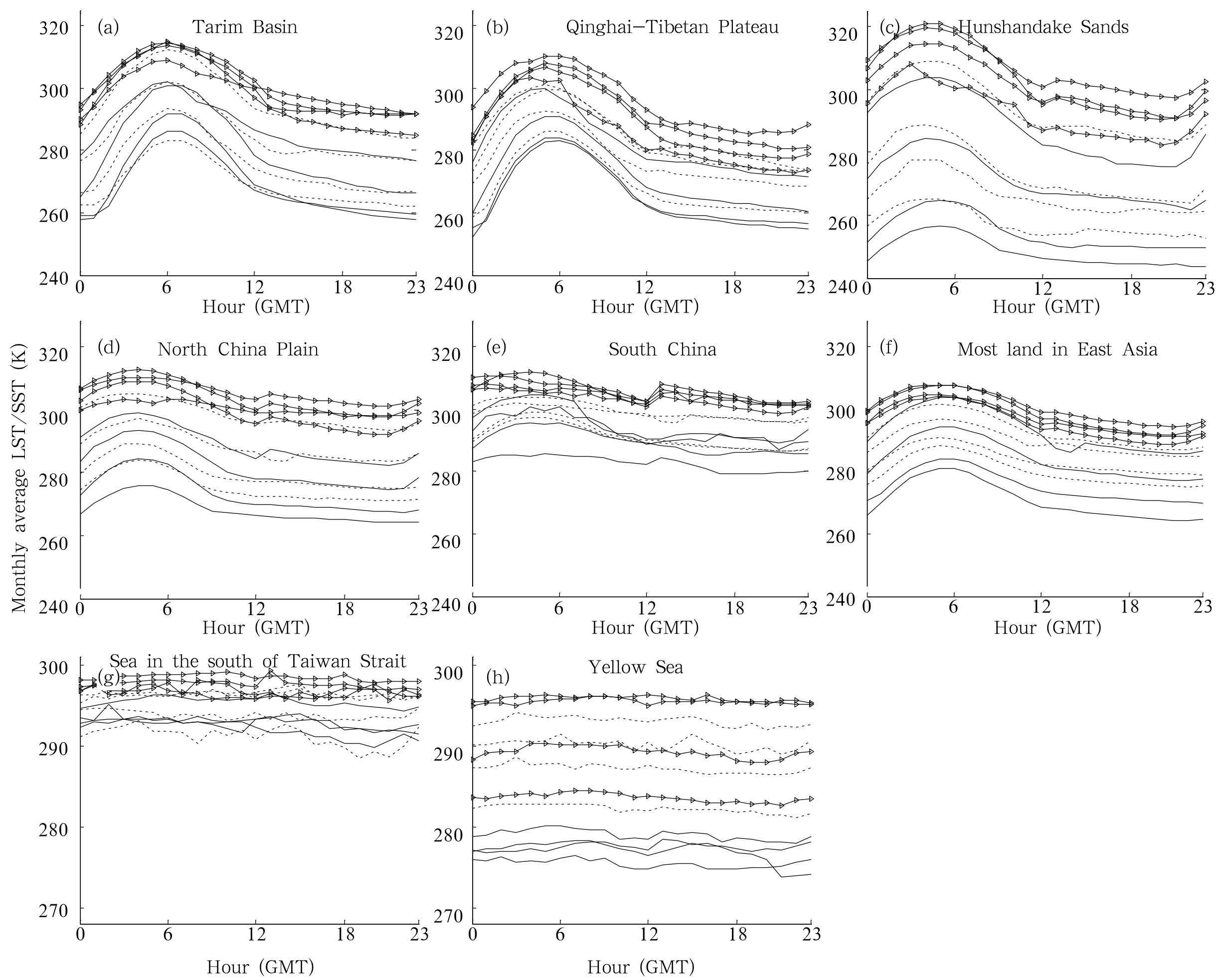

Fig.4. Diurnal cycle and seasonal variation of monthly average LST (K) in "pure" clear days in focused representative surface types in 2000. The x-coordinate is hour (GMT). (− Jan.-Apr.; −▷−May -Aug.; ⋯ Sep.-Dec.)

scattering degree indicates the diurnal and seasonal variation. Larger diurnal ranges in the Tarim Basin and Qinghai-Tibetan Plateau (both the surface types are mainly comprised of gravels or frozen soils) are because of less thermal capacity caused by lower water content in the soil, higher land surface albedo, therefore the land surface types are more sensitive to the solar radiation than others. In land surface types covered by dense vegetation throughout the entire year such as South China with abundant precipitation, high relative humidity on the ground, strong water absorbing ability/slow evaporation ability of the soil (agricultural farm and upland soil), the diurnal cycle of LST is not obvious. The diurnal cycle of monthly average SST is very slight, no more than 5 K at most.

In Fig.5, the amplitude of each curve shows the seasonal variation of LST/SST. Among several focused representative surface types, the seasonal variation of LST in Hunshandake Sands is the strongest with the largest amplitude, as also found in Fig.4 that the 12 curves are widely scattered. Seasonal variation of LST in the Qinghai-Tibetan Plateau is weaker with less amplitude, as shown in Fig.4 that the 12 curves are dense. The seasonal variation of LST in South China is weak. The seasonal variation of SST in Yellow Sea is a little stronger than that of the southern sea of Taiwan Strait, which obviously reveals the influence of the latitude.

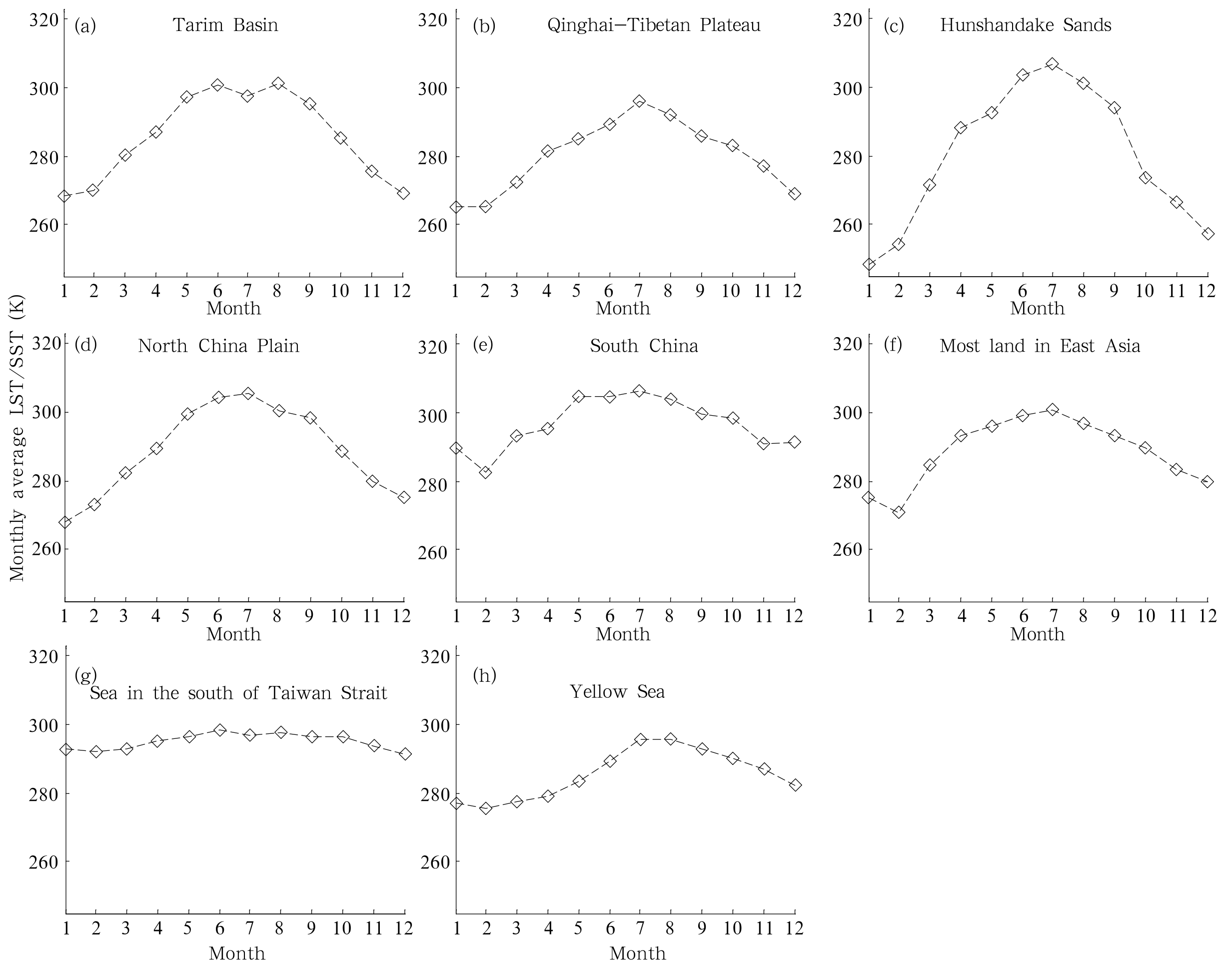

Fig.5. Seasonal variation of monthly average LST/SST (K) in "pure" clear days in focused representative surface types in 2000.

4.3 *Diurnal and annual range of LST in the representative land surface types in "pure" clear days in* 2000

Monthly average diurnal range of LST is defined as the LST difference between the maximum monthly average LST in a certain hour (usually at noon) in 24 h and the minimum monthly average LST in another hour (usually in the morning). Annual range of LST is defined as the LST difference between the maximum monthly average LST in a month of year and the minimum monthly average LST in another month.

The characteristics of seasonal variation of diurnal range of LST in the Tarim Basin, Hunshandake Sands, North China Plain, and most land in East Asia are shown in Fig.6. They have something in common: all show two peaks and two valleys. The maximum diurnal range of LST is in the spring (March-May) and the sub-valley is in September-October. Two valleys are in the summer (July-August) and December-January. These results are concerned with the long daytime, temporal distribution of precipitation and evaporation capacity of the soil surface in spring and summer in East Asia, which is located in the mid-latitude area of the Northern Hemisphere. In fact, diurnal range of LST depends on the sunlight intensity, short-wave albedo/long-wave emissivity, the inertia of land surface, and atmospheric water vapor content as well. Aerosol in the atmosphere plays a slight role. Figure 2 shows the maximum and minimum diurnal/annual ranges of LST/SST in the representative land/sea surface types and occurrence months in 2000. In the Qinghai-Tibetan Plateau and South China, the seasonal variation of diurnal range of LST is not obvious.

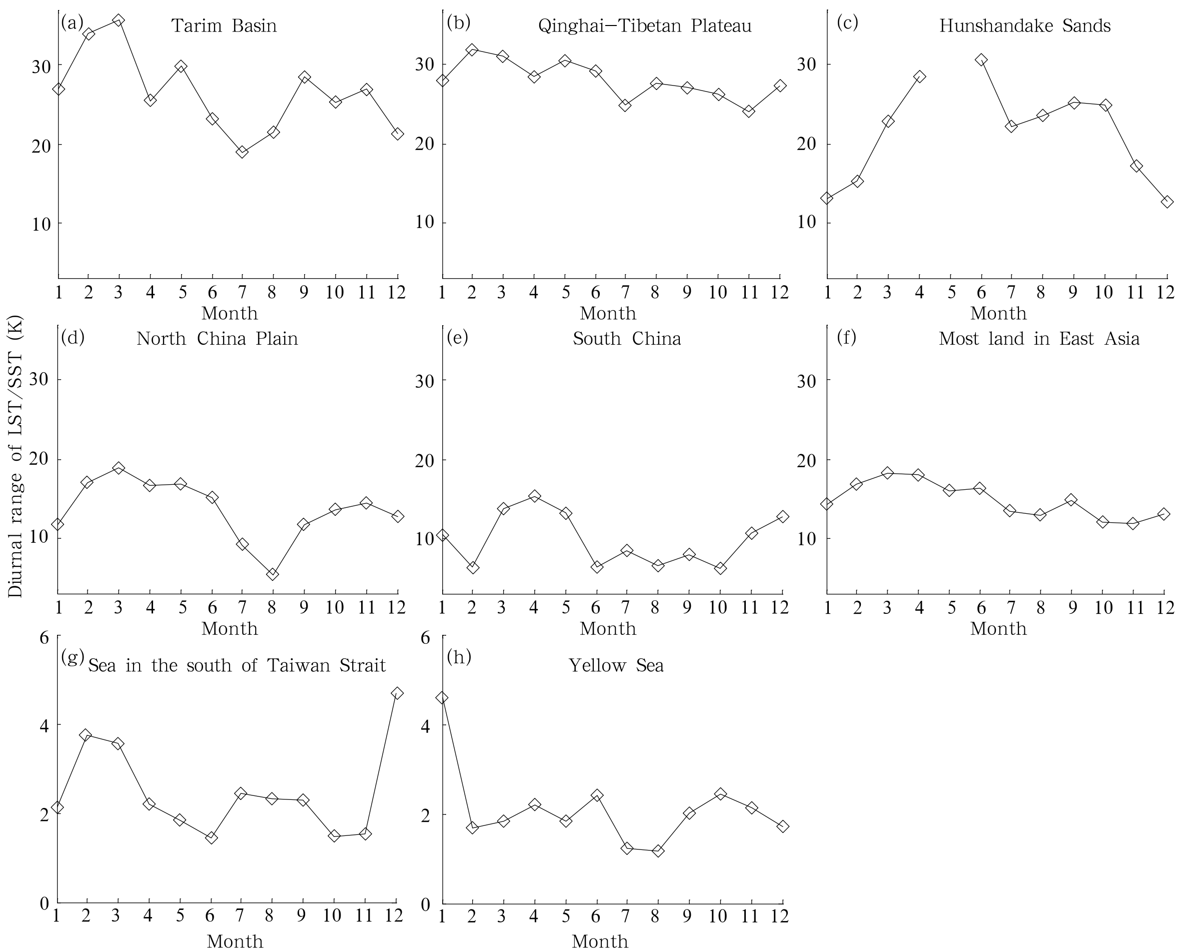

Fig.6. Seasonal variation of monthly average LST/SST (K) range in "pure" clear days in focused representative surface types in 2000.

When the amount of "pure" clear days and "pure" clear pixels are far more less in a period in some areas, the retrieved LST may have much larger bias from the real value, for less retrieved LST in real "pure" clear days. In Fig.6, the diurnal range of LST in Tarim Basin in May is unreasonably high due to possible influence of clouds. In May, there are only three "pure" clear days on May 1, 17, and 18, and only 4, 84, and 63 "pure" clear pixels respectively in the all 1876 pixels of the area. Hunshandake Sands has only 1 "pure" clear pixel in the all 348 pixels in the area on May 15, only 1 "pure" clear day in the month of May. In these circumstances, the retrieved LST does not represent average diurnal range of LST in a month. As a result, average diurnal/annual ranges of LST derived from the retrieved LST in the areas only have reference meaning.

The maximum diurnal range of LST (35.77 K) is in March in the Tarim Basin (with Taklimakan Desert), which is a result from the difference between 300.84 K at 07:00 GMT (hereinafter) and 265.07 K at 00:00. Jin (1997) indicates that diurnal range of LST in tropical and subtropical desert areas is the highest (Sahara Sands, July 1988). Although only the characteristics of diurnal range of LST worldwide in January and July are studied in Jin's paper, the result of spatial distribution of maximum diurnal range of LST is consistent with the result in this paper. LST at noon in summer is extremely high, e.g., monthly average LST at 06:00 in Tarim Basin in June and August are 314.44 and 313.41 K, respectively. Nevertheless, they are as low as 291.22 K at 22:00 in June and 291.89 K at 23:00 in August. Therefore, the maximum diurnal range of LST in these areas occurs in spring when solar radiation becomes stronger gradually and heat storage of land surface grows step by step, instead of in summer.

Despite larger diurnal ranges of LST in the Tarim Basin and North China Plain in March, average diurnal ranges of LST in these two areas are still lower than that in the Qinghai-Tibetan Plateau. The diurnal range of LST in the Qinghai-Tibetan Plateau is larger because of higher altitude and more short-wave solar radiation. In addition, due to less water vapor in the rarefied air, more infrared radiation from the ground toward the space, sparse vegetation and less precipitation, the widespread naked sand and stones absorbing and releasing heat rapidly, the diurnal range of LST is the largest among the several focused land surface types, especially in spring (Fig.4).

Table 2. Statistics data on LST/SST (K) in "pure" clear days in focused representative surface types in 2000

	Max. diurnal range	Month	Min. diurnal range	Month	Average diurnal range	Annual range	Month	Month
Tarim Basin	35.77	3	18.87	7	26.45	32.85	8	1
Qinghai-Tibetan Plateau	31.99	2	24.07	11	28.05	30.71	7	2
Hunshandake Sands	30.53	6	12.74	12	21.77	58.50	7	1
North China Plain	18.89	3	5.33	8	13.59	37.25	7	1
South China	15.32	4	6.17	10	9.80	23.47	7	2
Most land in East Asia	18.18	3	11.77	11	14.79	29.93	7	2
Sea in the south of Taiwan Strait	4.68	12	1.43	6	2.47	7.30	6	12
Yellow Sea	4.60	1	1.17	8	2.1	20.34	8	2

The surface layer comprises gravels mainly in Hunshandake Sands, where continental monsoon climate with medium drought style prevails. The annual precipitation is only 250-450 mm, much lower than evaporation capacity 1500-2000 mm, with the representative characteristic of coldness in winter and hotness in summer. Less water content in the soil results in higher land surface albedo. In case of rainfall, the water will infiltrate into the gravel layer rapidly, and the water in the surface layer will evaporate soon. The annual range of LST in this area is 57.50 K, much higher than those in other areas studied in this paper. The annual range in North China Plain ranks secondly, and that in the Tarim Basin is the third. Annual range of LST in most land in East Asia is 29.93 K. Monthly average LST in the Qinghai-Tibetan Plateau is the lowest in February, which is only 0.16 K lower than that in January. The characteristic of the highest

LST in July and lowest LST in January is consistent with the rule of highest air temperature in July and lowest air temperature in January in the inland areas of Northern Hemisphere.

LST and air temperature (average atmospheric temperature measured by dry-bulb thermometer in thermometer screen at a height of 1.5 m, a physical parameter to indicate the coldness and hotness of the air of the environment) are under the control of different physical factors, so they have different values and variations, diurnal ranges, seasonal ranges, and annual ranges, on which many experts made a lot of researches like Sun and Pinker (2003). Daily and annual average LST is higher than daily/annual air temperature, and diurnal range of LST is larger than that of air temperature, for the heat capacity of the atmosphere is much smaller than that of land surface. Here the comparison results are given to show the difference of LST and air temperature in China in 2000, with LST in different areas and the air temperature observed eight times per day in the stations around those areas (within 0.25 or 0.5 longitude and altitude scope), shown in Table 3. Due to the extremely asymmetric distribution of stations and less data from sparsely populated area such as the Qinghai-Tibetan Plateau, only some general conclusions can be drawn: except Tarim Basin, yearly average LST in several land surface types in the study is at least 2 K higher than yearly average air temperature. In most land in East Asia, yearly average LST is at least 4 K higher than yearly average air temperature.

Table 3. Comparison of yearly average LST (K) and air temperature (K) in neighboring stations in "pure" clear days in focused representative surface types in 2000

	Tarim Basin	Hunshandake Sands	North China Plain	South China	Most land in East Asia
Yearly average LST	285.69	279.79	288.71	296.71	288.51
Yearly average air Temperature (within 0.25°)	285.58	275.92	286.10	293.61	284.29
Number of stations (within 0.25°)	3	7	34	5	743
Yearly average air Temperature (within 0.5°)	285.29	275.92	285.81	293.93	284.30
Number of stations (within 0.5°)	7	7	39	9	747
$\overline{LST} - Ta^*$	273.54	277.02	275.84	276.17	277.95

Note: in the last row is the yearly average air temperature in 0.25° and 0.5°scopes.

4.4 *Characteristics of LST variation in "pure" clear days during* 1998-2000

Another work of this research is to establish a clear-day LST database (Wang and Lu, 2005a) by selecting suitable factors based on the single time/dual channel split-window algorithm. With the regression equation and the coefficient of the LST database, the parameters of LST in the representative land surface types in East Asia in "pure" clear days during 1998-2000 are calculated, and the characteristics of LST are analyzed.

LST has a slight increase in the three years, as Fig.7 shown, much more obviously in Hunshandake Sands. It is a little abnormal in East Asia in 1998 compared with the climate data. The time series of LST studied in this paper is not very long so that it is hard to find out the continuous, steady rules of LST variation in multi-year scale. Sands, plain, basin, plateau, and mountain areas have a decreasing degree of LST seasonal variation one after another, the feature of LST seasonal variation is the same as that in 2000.

A rule of two peaks and two valleys is also typical in the diurnal range of LST during 1998-2000 (Fig.8). The comparison of the monthly average diurnal range of LST in the same month among the three years shows a slight decline trend, because the maximum

LST (monthly average LST in 1 h) declines gradually while the minimum LST rises gradually, and the latter plays a more decisive role. Decline trend of diurnal range of LST results from the climate reason like the variation of heat and water exchange between soil and vegetation caused by greenhouse effect, air pollution and human activities, etc.

5. Difference analysis of LST parameters in Hunshandake Sands and Xilinguole typical grassland

Xilinguole typical grassland (43.5°-45°N, 113°-116.31°E) on the north of Hunshandake Sands (42.1°-43.5°N, 113°-116.31°E) is a typical transitional belt in China from grassland to desert steppe, where there are mainly meadow grassland, typical grassland, and desert steppe. The human activities such as overgrazing in the past decades have deprived Xilinguole typical grassland of its previous legend of "flocks and herds looming in the grassland". Now it consists of sparse meadow mainly, even deserts in some areas. Comparatively, Hunshandake Sands has less vegetation coverage than its northern Xilinguole typical grassland. The distribution of sands, grassland, and lakes in Hunshandake Sands is more complicated than that in the northern grassland (Lu et al., 2002).

The results in Table 4 and Fig.9 (monthly average LST and diurnal range of LST in Hunshandake Sands in May only works as reference because of less "pure" clear pixels) show that monthly average LST in Hunshandake Sands in "pure" clear days is slightly higher than that in the northern grassland. Seasonal variations of diurnal range of LST in these two areas are a typical two-peak and two-valley type. In June,

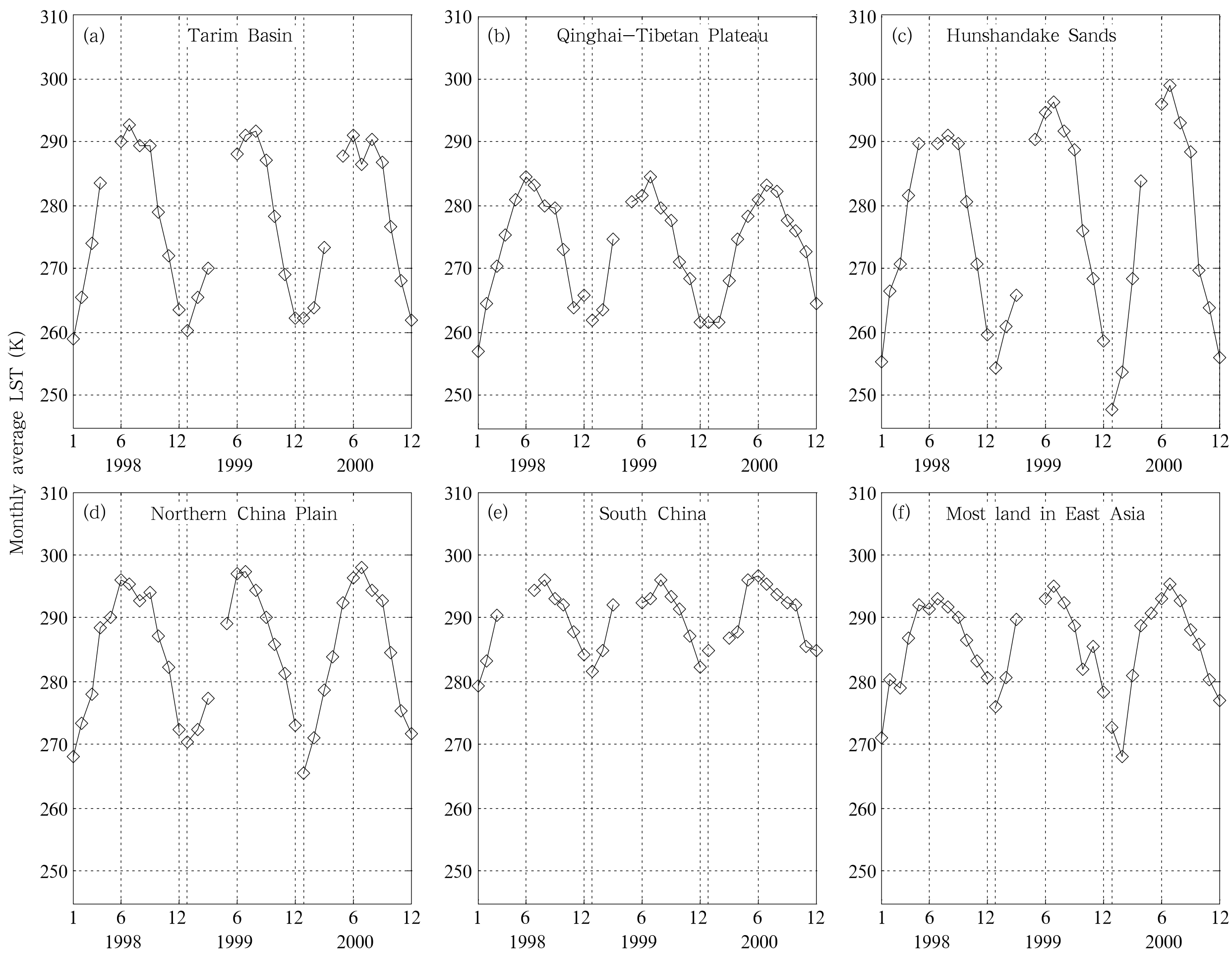

Fig.7. Annual variation of LST/SST in "pure" clear days in focused representative surface types in 1998-2000 (K).

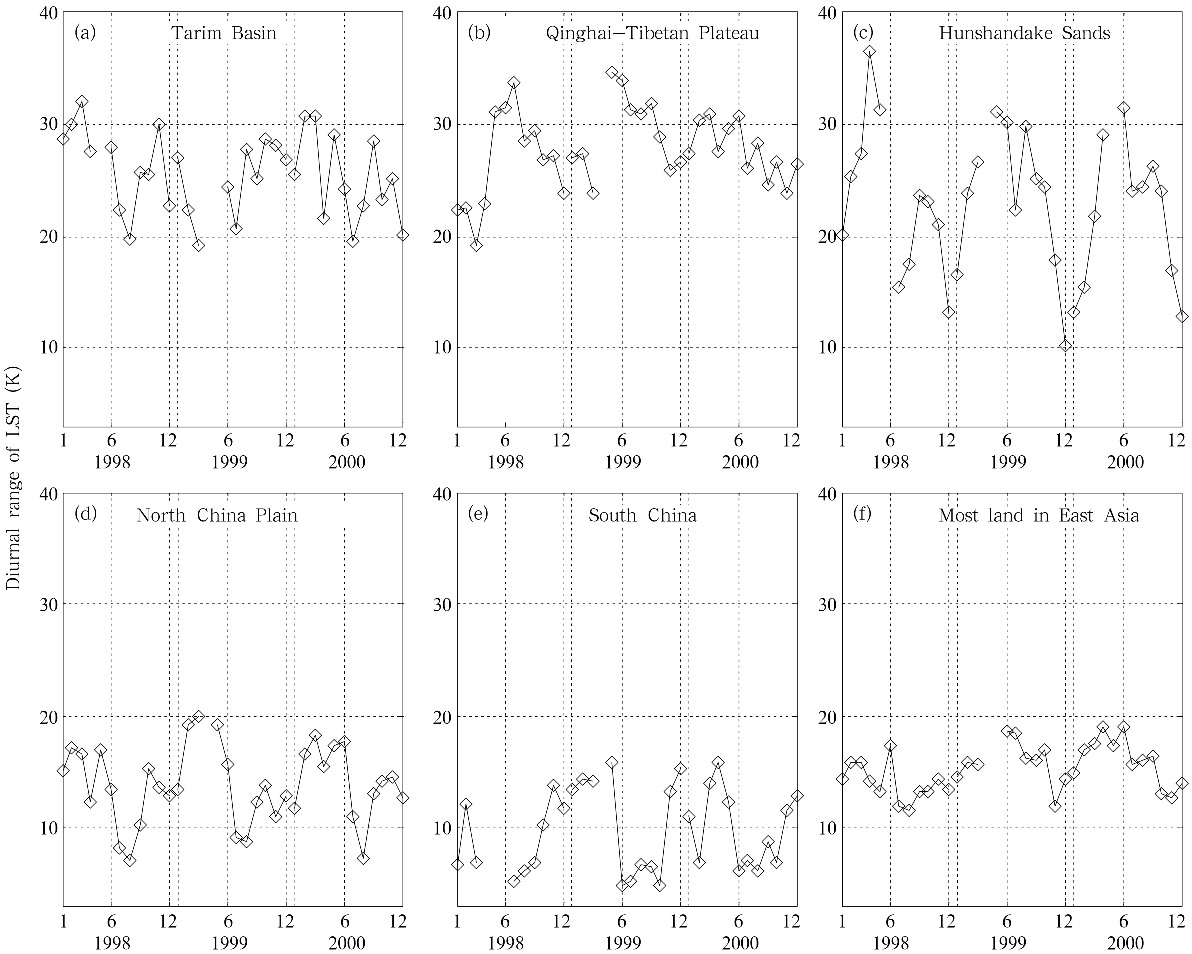

Fig.8. Annual variation of LST/SST range in "pure" clear days in focused representative surface types in 1998-2000 (K).

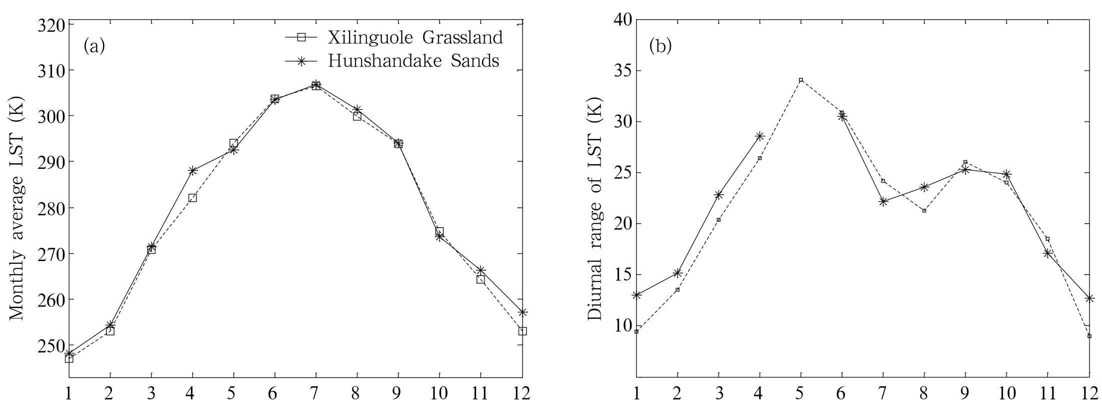

Fig.9. Seasonal variation of monthly average LST and monthly LST range in Hunshandake Sands and Xilinguole typical grassland in "pure" clear days in 2000 (K).

July and November, diurnal range of LST in Hunshandake Sands is less than that in the northern grassland. Diurnal range of LST in Hunshandake Sands has a weaker valley in July while that in the northern grassland is one month later (August). The yearly average LST of Xilinguole typical grassland is 278.26 K. From these results, a trend of degradation is obvious in the northern grassland.

These results are directly related to the selection of "pure" clear days in cloud detect algorithm. There are only 7 and 4 "pure" clear days in Hunshandake Sands in July and August, respectively, and only 9 and 5 "pure" clear days in Xilinguole typical grassland in July and August, respectively.

Table 4. The difference of LST parameter between Hunshandake Sands and Xilinguole grassland in "pure" clear days in 2000 (K)

	Max. diurnal range	Month	Min. diurnal range	Month	Yearly average diurnal range	Annual range	Month	Month
Xilinguole typical grassland	34.07	5	8.98	12	21.47	59.49	7	1
Hunshandake Sands	30.53	6	12.74	12	21.77	58.50	7	1

6. Conclusions

GMS5/VISSR observation with 1-h temporal resolution is a good dataset to study meso/micro-scale physical parameters in the earth-atmosphere system. LST plays an important role in remote sensing of the environment and the study of earth resources. That is one of the reasons for LST to be one of the popular focuses in remote sensing field in recent decades of years. The diurnal and seasonal variation of LST reflects not only the influence of solar radiation on the earth surface and the lower atmosphere in different geographic conditions but also reveals various physical properties of surface types themselves.

The single time/dual channel split-window algorithm is adopted to retrieve LST in this paper. The characteristics of diurnal and seasonable variation of LST in several representative land surface types (Tarim Basin, Qinghai-Tibetan Plateau, Hunshandake Sands, North China Plain, and South China) in "pure clear days" are discussed. LST parameters in most land in East Asia are also studied as comparison. Moreover, Sea Surface Temperature and relevant characteristics in the south of Taiwan Strait and Yellow Sea are listed in this paper. The variation characteristic of LST in 2000 is emphasized in this paper. The variation characteristic of LST during 1998-2000 is also shown, in which the regression equation for the establishment of LST database derived from Wang and Lu (2005b) is directly used.

All these results are valuable to the studies of climate change, radiation balance, and estimation for the change of land surface types.

(1) In most land in East Asia, LST reaches the highest in 05:00 GMT and lowest in 21:00, and the variation of LST at night is much lower than in daytime. The land of East Asia in mid-latitude has an obvious LST feature: warm in summer while cold in winter.

(2) In the Tarim Basin, Hunshandake Sands, North China Plain, and most land in East Asia, the monthly average diurnal range of LST in 2000 shows two peaks and two valleys. The peak and sub-peak of diurnal range occur in spring (March-May) and autumn (September-October), respectively, and two valleys of diurnal range occur in summer (July-August) and winter (December-January), respectively. Tarim Basin and Hunshandake Sands, under the impact of the geographical factors and long-term climate variation (located in the drought/semi-drought zone, precipitation obviously lower than other areas at the same latitude), not only have considerable LST diurnal cycle but also have remarkable seasonal variation due to high reflectivity of the land surface, rapid heat conduction of soil, and water evaporation of land surface. The maximum diurnal ranges of LST in those two areas reach 35.77 and 30.53 K in 2000, respectively. Annual range of LST in Hunshandake Sands is up to

58.50 K in 2000. Seasonal variation of LST in the Qinghai-Tibetan Plateau is not very high while the diurnal range is large, yearly average diurnal range in 2000 is 28.05 K.

(3) Results show that there is a rising trend of LST in East Asia during 1998-2000, especially in Hunshandake Sands. A slight decline of diurnal range of LST is caused by the slight decline of maximum LST and slight increase of minimum LST.

(4) LST parameters in Hunshandake Sands and its northern Xilinguole typical grassland are not discrepant.

Acknowledgments. We would like to thank Prof. Mao Jietai in Department of Atmospheric Science, Peking University, for providing GMS5 data and cloud detection algorithm; Beijing Meteorological Bureau, from which we get in-situ 0-cm observation of surface temperature at Station No. 54511; National Meteorological Information Center of Chinese Meteorological Administration, from which we get the dataset of surface temperature in other national reference climatological stations in China.

REFERENCES

Becker, F., and Li Z. L., 1990: Towards a local split window method over land surface. *International Journal of Remote Sensing*, **11**, 369-394.

Becker, F., and Li Z. L., 1995: Measurement of Land Surface Temperature and Emissivity from Space: Methods, Results and Related Problems. The 6th International Colloquium-Physical Measurements and Signatures in Remote Sensing, Val d'Isère (France), January 17-21.

Faysash, D. A., and E. A. Smith, 1999: Simultaneous land surface temperature-emissivity retrieval in infrared split window. *Journal of Atmospheric and Oceanic Technology*, **16**, 1673-1689.

Jin, M. L., 1997: A comparison of CCM2-BATS skin temperature and surface-air temperature with satellite and surface observations. *Journal of Climate*, **10**, 1505-1524.

Lu Daren, Chen Zuozhong, Chen Jiayi, et al., 2002: Composite study on Inner Mongolia semi-arid grassland soil-vegetation-atmosphere interaction (IMGRASS). *Earth Science Frontiers (China University of Geosciences)*, **9**, 295-306. (in Chinese)

Mao Jietai, Wang Meihua, Mao Yali, et al., 1999: Probability distribution of clear astronomical night in China. *Acta Astrophysica Sinica*, **19**(4), 432-446. (in Chinese)

McClain, E. P., W. G. Pichel, and C. C. Walton, 1985: Comparative performance of AVHRR based multichannel sea surface temperatures. *Journal of Geophysical Research*, **90**(c6), 11587-11601.

Oku, Y., and H. Ishikawa, 2004: Estimation of land surface temperature over the Tibetan Plateau using GMS data. *Journal of Applied Meteorology*, **43**, 548-561.

Prata, A. J., and R. P. Cechet, 1999: An assessment of the accuracy of land surface temperature determination from the GMS 5 VISSR. *Remote Sens. Environ.*, **67**, 1-14.

Prata, A. J., and C. M. R. Platt, 1991: Land surface temperature measurements from the AVHRR. Proceeding of the 5th AVHRR Data Users Meeting, Tromso (Norway), June 25-28, EUM P09, 433-438.

Price, J. C., 1984: Land surface temperature measurements from the split window channels of the NOAA 7 advanced very high resolution radiometer. *Journal of Geophysical Research*, **89**(5), 7231-7237.

Sobrino, J. A., and N. Raissouni, 2000: Toward remote sensing methods for land cover dynamic monitoring: Application to Morocco. *Remote Sensing*, **21**(2), 353-366.

Sun Donglian and R. T. Pinker, 2003: Estimation of land surface temperature from a Geostationary Operational Environmental Satellite (GOES-8). *Journal of Geophysical Research*, **108**(D11), 4326-4341.

Ulivieri, C. M. M., R. F. Castromuovo, et al., 1994: A split-window algorithm for estimation land surface temperature from satellites. *Advances in Space Research*, **14**, 59-65.

Wang Minyan and Lu Daren, 2005a: Land surface temperature database in clear days retrieved by using GMS5 satellite observation: Preliminary investigation. Proceeding of SPIE, Optical Technologies for Atmospheric, Ocean, and Environmental Studies, Vol. 5832, Part II: 420-430.

Wang Minyan and Lu Daren, 2005b: An improved algorithm to retrieve land surface temperature by GMS 5 data. *Chinese Journal of Geophysics*, **48**(5), 1034-1044.

Yan Hao, Wang Changyao, Niu Zheng, et al., 2001: Comparative studies of China temperature change by using remote sensing and traditional data. *Climate and environment research*, **6**(4), 448-455. (in Chinese)